Ferroelectric states induced by dimer lattice disorder in dimer Mott insulators

Hiroki Gomi,[1,2] Masahiro Ikenaga,[3] Yasuhiro Hiragi,[3] Daiki Segawa,[3] Akira Takahashi,[1,2]
Takeshi J. Inagaki,[3] and Masaki Aihara[3]

[1]*Graduate School of Engineering, Nagoya Institute of Technology, Gokiso-Cho, Showa-ku, Nagoya 466-8555, Japan*
[2]*CREST, Japan Science and Technology Agency, Chiyoda-ku, Tokyo 102-0075, Japan*
[3]*Graduate School of Materials Science, Nara Institute of Science and Technology, Ikoma, 630-0192, Japan*

(Received 30 December 2012; revised manuscript received 16 April 2013; published 21 May 2013)

We theoretically investigate the dielectric properties of dimer Mott insulators. We adopt the two-dimensional quarter-filled extended Hubbard model for κ-(BEDT-TTF)$_2X$ that includes the coupling with the dimer lattice modes, and numerically calculate the ground state for the bond-length-alternated and disordered lattices. Electric dipole moments in dimers are induced by interdimer bond-order alternation, and electric dipole moments are aligned perpendicular to the direction of bond-order alternation. As a result, the electric polarizations arising from electric dipole moments in dimers are strongly coupled with the dimer lattice modes of interdimer bond-length alternation, and the more stable one of these two ferroelectric states is induced by disorder in dimer lattice. The ferroelectric states arise from the hybridization of in-gap charge excited states to the dimer Mott ground state for the equilibrium lattice, and one (the other) is strongly stabilized near the phase boundary with the metallic phase (in the spin-liquid phase). The present results are consistent with the experimentally observed dielectric anomaly in κ-(BEDT-TTF)$_2$Cu$_2$(CN)$_3$.

DOI: 10.1103/PhysRevB.87.195126 PACS number(s): 77.80.−e, 71.30.+h, 78.30.Jw

I. INTRODUCTION

The ferroelectricity where electric polarization is governed by electrons is termed electronic ferroelectricity.[1,2] In electronic ferroelectricity, a large magnetodielectric coupling and a fast polarization switching are expected, and electronic ferroelectricity has attracted much attention because of these novel properties. Multiferroic[3–5] (where the ferroelectricity is driven by spin ordering) and charge-order-driven (where electric polarization is caused by an electronic charge order without inversion symmetry) ferroelectricity are representative examples of electronic ferroelectricity. In this paper, we focus on the latter one. The charge-order-driven ferroelectricity has been observed in inorganic transition-metal oxides $LuFe_2O_4$,[6–8] as well as organic charge-transfer salts (TMTTF)$_2X$ (X = a monovalent cation)[9–11] and α-(BEDT-TTF)$_2$I$_3$.[12]

Recently, dielectric anomaly has been observed in dimer Mott insulators κ-(BEDT-TTF)$_2$Cu$_2$(CN)$_3$ (Ref. 13) and β'-(BEDT-TTF)$_2$ICl$_2$ (Ref. 14), and this shows the possibility of electronic ferroelectricity in these materials. In (BEDT-TTF)$_2X$ (X = a monovalent anion), the crystal structure consists of alternating stacking of BEDT-TTF and counter anion layers, and the BEDT-TTF layers dominate their low-energy properties. Since there is one hole per two BEDT-TTF molecules, (BEDT-TTF)$_2X$ can be described as quasi-two-dimensional strongly correlated electron systems with a quarter-filled valence band. In κ-(BEDT-TTF)$_2X$, the BEDT-TTF molecular lattice is distorted to form dimers, and the two sites that are hybridized can be effectively treated as a single site. Since there is one hole per dimer site, the valence band becomes half-filled as a result of the dimerization. As a result, κ-(BEDT-TTF)$_2X$ exhibits the Mott insulator phase if $U^{(\mathrm{dim})}$ is larger than its critical value, where $U^{(\mathrm{dim})}$ is the Coulomb interaction energy between the two holes in a dimer.[15–18] Since the Mott insulator phase is stabilized by dimerization, the state is called the dimer Mott insulator.

In κ-(BEDT-TTF)$_2X$, the dimer sites form an anisotropic triangular lattice. The strong correlation and the geometrical frustration act cooperatively to generate exotic phases such as a quantum spin-liquid state.[19] The possibility of quantum spin-liquid states is proposed in κ-(BEDT-TTF)$_2$Cu$_2$(CN)$_3$ because of the absence of a long-range magnetic order down to 32 mK.[20–23] It is considered that the dimer sites form a nearly regular triangular lattice in the material,[24] and the origin of the quantum spin-liquid states has been ascribed to the geometrical frustration effect from the triangular lattice. Various theoretical works have been done on this problem using a half-filled Hubbard model on a triangular lattice, and some of them have succeeded to show a nonmagnetic and gapless state becomes the ground state in a parameter range of anisotropy.[25–29]

The dielectric anomaly strongly suggests that charge degrees of freedom are still active in the dimer Mott insulators κ-(BEDT-TTF)$_2$Cu$_2$(CN)$_3$. Aside from the dielectric anomaly, several results that are considered to result from charge degrees of freedom have been obtained: optical components that are considered to be electronic origin exist inside the Mott gap,[30–32] the broadening of some vibrational modes,[33–35] and anomalies in the lattice expansion coefficient and specific heat at around 6 K.[36,37] The origins of these phenomena have been intensely discussed, and it is proposed that they arise from electric dipole moments in dimers.[13,14,30–32,38,39] On the other hand, there are experimental results that show the absence of electric dipole moments in dimers,[40,41] and it is still controversial as to whether the electric dipole moments in dimers exist or not.

Most of the theoretical works on κ-(BEDT-TTF)$_2X$ have been done using the half-filled model, where a dimer is considered as a unit and intradimer degrees of freedom are neglected. Recently, several theoretical works have been done using the quarter-filled model, where a BEDT-TTF molecule is considered as a unit and intradimer degrees of freedom are taken into account, to challenge this problem. Naka and

Ishihara,[38] and Hotta[39] have derived the effective Hamiltonians for the quarter-filled extended Hubbard model for κ-(BEDT-TTF)$_2X$ assuming that the Hilbert space is restricted to states with one hole per dimer, and they have succeeded to show that the ferroelectric phase arising from electric dipole moments in dimers is realized in some parameter ranges. Furthermore, the interactions between the electric dipoles and spins are included in these models, and the effects of dipolar-spin coupling on the spin structure is discussed in these works. We have found that ferroelectric state arising from electric dipole moments in dimers becomes the ground state near the phase boundary between the dimer Mott insulator and metallic phases in the quarter-filled extended Hubbard model for κ-(BEDT-TTF)$_2X$.[30] The electric dipoles in dimers are generated by bond-order alternation, which can not be described in the effective models for the strong-coupling case. A similar ferroelectric state is found in the model with different lattice structure with strong geometrical frustration.[42] However, it is not still clear whether the origins of these ferroelectric states in the original and the effective models are the same.

The dielectric constant exhibits the characteristic temperature dependence in κ-(BEDT-TTF)$_2$Cu$_2$(CN)$_3$.[13] However, the origin of the temperature dependence is not yet understood well. To consider the origin of the dielectric anomaly, it is essential to investigate the effect of heat. Furthermore, the ferroelectric states induced by bond-order alternation are strongly coupled with dimer lattice motion. We therefore investigate the effect of disorder in the positions of dimers, which arises from heat, on the charge and spin structures of dimer Mott insulators in this paper. Furthermore, the ferroelectric states found in the effective models are stabilized by the interdimer Coulomb interaction, and the ferroelectric phase exists in the vicinity of the phase boundary with the charge-ordered phase.[38,39,43] We therefore analyze the dependence of the effects of disorder on the interdimer Coulomb interaction energies in detail to consider the origins of the ferroelectric states.

II. MODEL

To take account of the intradimer degrees of freedom, a dimer is not considered as a unit but a BEDT-TTF molecule is regarded as a lattice site. We consider only a lowest unoccupied molecular orbital (LUMO) of a BEDT-TTF molecule because it dominates the low-energy physics of κ-(BEDT-TTF)$_2X$. Therefore, there is one orbital for a lattice site, and the electron system is quarter-filled in terms of holes. We consider the quarter-filled extended Hubbard Hamiltonian for holes on a two-dimensional anisotropic triangular lattice. It is given by

$$H = \sum_{\langle n,m\rangle} \beta_{n,m}\hat{p}_{n,m} + U\sum_{n} n_{n,\uparrow}n_{n,\downarrow} + \sum_{\langle n,m\rangle} V_{n,m}n_n n_m. \quad (1)$$

The first term describes the transfer of holes, where $\langle n,m\rangle$ denotes neighboring site pairs, $c_{n,\sigma}$ ($c^{\dagger}_{n,\sigma}$) is the annihilation (creation) operator for a hole with the spin σ at the site n, $\beta_{n,m}$ is the transfer integral between the sites n and m, $\hat{p}_{n,m}$ is the bond-order operator for the bond between the sites n and m, and it is given by

$$\hat{p}_{n,m} = \sum_{\sigma}(c^{\dagger}_{m,\sigma}c_{n,\sigma} + c^{\dagger}_{n,\sigma}c_{m,\sigma}). \quad (2)$$

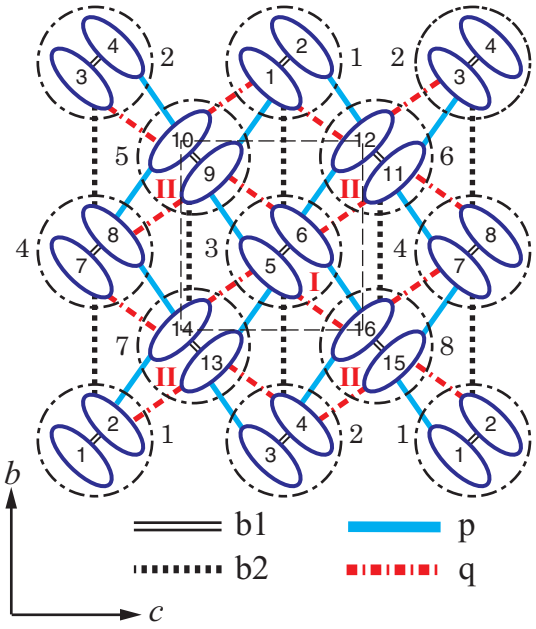

FIG. 1. (Color online) Lattices structure of κ-(BEDT-TTF)$_2X$ looking along the molecular axis. The ellipsoids show BEDT-TTF molecules, and the numbers in ellipsoids show the site numbers. The circles show the dimers, and the dimer numbers are shown near the circles. The rectangle denotes a unit cell.

The second and the third terms describe the onsite Coulomb interaction and the Coulomb interaction between the neighboring sites, respectively, where U is the onsite Coulomb interaction energy, $V_{n,m}$ is the Coulomb interaction energy between the sites n and m, $n_{n,\sigma} = c^{\dagger}_{n,\sigma}c_{n,\sigma}$, and $n_n = \sum_{\sigma} n_{n,\sigma}$.

We show the lattices structure of κ-(BEDT-TTF)$_2X$ in Fig. 1. As shown in the figure, there are four nonequivalent bonds, and they are labeled by b1, b2, p, and q according to Mori *et al.*[44] The b1 bond is much stronger than the other ones, and the two BEDT-TTF molecules connected by the b1 bond form a dimer. We consider the 4×4 cluster of the system size $N = 16$, and the periodic boundary condition is used. The shape of the cluster is shown in Fig. 1. There are three different periodic boundary conditions. In the periodic boundary condition I (II), the 16-site clusters are tiled in a staggered manner along the c axis (b axis) to cover the anisotropic triangular lattice, where we adopt the crystal axes for κ-(BEDT-TTF)$_2$Cu$_2$(CN)$_3$, and the b and c axes are defined as shown in Fig. 1. In the condition III, the clusters are tiled without staggering. We show the results with the condition I shown in Fig. 1 in this paper because interdimer networks of important p and b1 bonds are the longest in the case. We check the finite-size effect by analyzing how the present results depend on the periodic boundary condition. They are not altered qualitatively by changing the periodic boundary conditions, showing that the finite-size effect is not serious for the results shown in this paper.

We consider the displacements of dimer positions on the b-c plain. The change in the b1 bond lengths and the lattice deviations along the the molecular axis (a axis) are not considered in this paper because their effects are significantly smaller than those considered here. We denote the c-axis

(b-axis) component of the position vector of the site n by x_n (y_n), that for the equilibrium position of the site n by $\bar{x}_n$ ($\bar{y}_n$), and the deviations by $\Delta x_n = x_n - \bar{x}_n$ and $\Delta y_n = y_n - \bar{y}_n$. We define the site and the dimer numbers so that the sites $2l-1$ and $2l$ constitute the dimer l as shown in Fig. 1. Since only deviations of dimer positions are considered, it is assumed that $\Delta x_{2l-1} = \Delta x_{2l}$ and $\Delta y_{2l-1} = \Delta y_{2l}$ hold.

Both $\beta_{n,m}$ and $V_{n,m}$ depend on the relative position between the two sites n and m. We consider small deviations, and take account of the dependence of $\beta_{n,m}$ on Δx_n and Δy_n only to the first order. Furthermore, since $V_{n,m}$ weakly depends on them, we assume that $V_{n,m}$ does not depend on Δx_n and Δy_n. Then, the interdimer transfer integrals are given by

$$\beta_{n,m} = \bar{\beta}_{n,m} + (\bar{\beta}_{n,m})_x \mathrm{sgn}(\bar{x}_n - \bar{x}_m)(\Delta x_m - \Delta x_n) + (\bar{\beta}_{n,m})_y \mathrm{sgn}(\bar{y}_n - \bar{y}_m)(\Delta y_m - \Delta y_n), \quad (3)$$

where $\bar{\beta}_{n,m}$ are the transfer integrals for the equilibrium arrangement, $(\bar{\beta}_{n,m})_x$ and $(\bar{\beta}_{n,m})_y$ are the differential coefficients of $\beta_{n,m}$, and $\mathrm{sgn}(x)$ shows the sign of x. We denote $\bar{\beta}_{n,m}$, $(\bar{\beta}_{n,m})_x$, $(\bar{\beta}_{n,m})_y$, and $V_{n,m}$ for the b1 bond by $\bar{\beta}_{\mathrm{b1}}$, $(\bar{\beta}_{\mathrm{b1}})_x$, $(\bar{\beta}_{\mathrm{b1}})_y$, and V_{b1}, respectively. Those for other quantities and those for the other bonds are denoted in the same way.

In this paper, we use a single differential coefficient β' assuming that $(\bar{\beta}_{\mathrm{p}})_x = (\bar{\beta}_{\mathrm{p}})_y = \beta'$, $(\bar{\beta}_{\mathrm{q}})_x = (\bar{\beta}_{\mathrm{q}})_y = -\beta'$, $(\bar{\beta}_{\mathrm{b2}})_x = 0$, $(\bar{\beta}_{\mathrm{b2}})_y = \beta'$. Here, since $\bar{\beta}_{\mathrm{p}} > 0$, $\bar{\beta}_{\mathrm{q}} < 0$, and $\bar{\beta}_{\mathrm{b2}} > 0$ hold, negative coefficients are assumed for the q bond. Moreover, since the b2 bonds are nearly parallel to the b axis, we set $(\bar{\beta}_{\mathrm{b2}})_x = 0$. Qualitatively, the same results are obtained when different differential coefficients are used for different bonds as long as the differences are not so large. We calculate the ground state $|\psi_0\rangle$ of H by the Lanczos method. To investigate the physical properties of $|\psi_0\rangle$, we numerically calculate the charge density $\rho_n = \langle\psi_0|n_n|\psi_0\rangle - 0.5$, the charge correlation function $\xi_{n,m} = \langle\psi_0|(n_n - 0.5)(n_m - 0.5)|\psi_0\rangle$, the spin correlation function $\eta_{n,m} = \langle\psi_0|\boldsymbol{S}_n \cdot \boldsymbol{S}_m|\psi_0\rangle$, where $\boldsymbol{S}_n$ is the spin operator at the site n, and the probability W_{s} that a dimer is singly occupied in $|\psi_0\rangle$.

III. RESULTS

A. Regular case

In this section, we show the results for the equilibrium lattice, where $\Delta x_n = \Delta y_n = 0$ holds. To estimate the reasonable parameters for κ-(BEDT-TTF)$_2X$, we calculate the ground state in a wide range of parameter space. We find only two phases in the realistic parameter range, and the considered physical quantities discontinuously change at the boundary. In one phase, the spin correlation is always negative between the dimers I and II, where there are two dimers in the unit cell, and they are labeled by I and II as shown in Fig. 1. This shows that the phase has antiferromagnetic (AFM) spin order. The other phase is paramagnetic (PM) because the magnitudes of spin correlations are much smaller than those for the AFM phase. Since the PM ground state has an overlap as large as about 0.8 with one of the degenerate metallic ground states in the noninteracting case of $U = V_{\mathrm{b1}} = V_{\mathrm{b2}} = V_{\mathrm{p}} = V_{\mathrm{q}} = 0$, we can conclude that the state is metallic. The AFM spin order shows the localization of holes. Furthermore, W_{s} in the AFM phase is close to 1 and it is significantly larger than that in the PM phase. These results show that the AFM state is a dimer Mott insulator. We can not show the existence of the spin-liquid phase from the present results in small-size cluster. However, the dimer Mott insulator ground state always has the strong AFM spin order, and this suggests that the spin-liquid phase is not found in the parameter region shown in this paper.

As will be shown later, the charge structure of the disordered ground state sensitively depends on the interdimer Coulomb interaction energies V_{b2}, V_{p}, and V_{q}. The charge structure depends also on the other parameters. However, the dependence can be understood through two quantities Δe and $\Delta e'$ unless quite different values are used. Here, Δe is the energy difference per site of the metallic phase from the the dimer Mott insulator phase, and $\Delta e'$ is that of a different dimer Mott insulator phase from the ground state, which will be described later. The effects of disorder become stronger as Δe or $\Delta e'$ decreases, and they are strongly enhanced near the phase boundaries. We therefore mainly investigate the dependence of the ground-state properties on V_{b2}, V_{p}, V_{q} in this paper, and adopt $\bar{\beta}_{\mathrm{b2}}$ as the parameter that controls Δe and $\Delta e'$.

The transfer integrals for κ-(BEDT-TTF)$_2$Cu[N(CN)$_2$]Br are calculated by the extended Hückel method, and they are given by $\bar{\beta}_{\mathrm{b1}} = 0.265$, $\bar{\beta}_{\mathrm{b2}} = 0.098$, $\bar{\beta}_{\mathrm{p}} = 0.109$, and $\bar{\beta}_{\mathrm{q}} = -0.038$.[44] Here and hereafter, we use eV as the unit of energy. We adopt them except for $\bar{\beta}_{\mathrm{b2}}$. The onsite Coulomb interaction energy is estimated from the Knight shift,[15,16] and we adopt this value $U = 0.7$. The estimated values for the Coulomb interaction energies between the neighbor sites are 0.27 eV $\sim$ 0.35 in the cases of α-(BEDT-TTF)$_2$I$_3$ and θ-(BEDT-TTF)$_2$RbZn(SCN)$_4$ without dimerization.[45,46] It is expected that V_{b1} is larger, and V_{b2}, V_{p}, and V_{q} are smaller than these values in the dimerized present case. We therefore adopt the value $V_{\mathrm{b1}} = 0.45$. The values for on-dimer Coulomb interaction energy $U^{(\mathrm{dim})}$, which is determined from U, V_{b1} and $\bar{\beta}_{\mathrm{b1}}$, obtained in various references are largely different.[17–19,47,48] However, qualitatively the same results are obtained with using quite different values of $U^{(\mathrm{dim})}$ as long as the ground state is the dimer Mott insulator. This point will be discussed later.

We mainly consider κ-(BEDT-TTF)$_2X$ near the phase boundary between the dimer Mott insulator and the metallic phase, and we use the value $\bar{\beta}_{\mathrm{b2}} = 0.073$ that gives very small Δe. For $V_{\mathrm{b2}} = V_{\mathrm{p}} = V_{\mathrm{q}} = 0.25$, the ground state is a dimer Mott insulator (a metallic state) for $\bar{\beta}_{\mathrm{b2}} \leqslant 0.073$ ($\bar{\beta}_{\mathrm{b2}} \geqslant 0.074$). We show spin and charge correlation functions for the various values of V_{q} in Fig. 2. The other interdimer Coulomb interaction energies are fixed to the values $V_{\mathrm{b2}} = 0.25$ and $V_{\mathrm{p}} = 0.25$. Here, the results with unrealistic values of V_{q} are included because they will help us to understand the ground-state properties in the realistic parameter region.

Since all the sites are equivalent, the correlations at all the site pairs are included in these figures. As seen from Fig. 2(b), the charge correlation function changes remarkably with V_{q}. For $V_{\mathrm{q}} = 0.4$, $\xi_{n,m} > 0$ ($\xi_{n,m} < 0$) holds for the site pairs with the same color (different colors) shown in Fig. 3(a). This shows that the charge structure shown in Fig. 3(a), where electric dipole moments in dimers are generated and they are aligned along the b axis, is the dominant charge fluctuation in this case. For $V_{\mathrm{q}} = 0$, $\xi_{n,m} > 0$ ($\xi_{n,m} < 0$) holds for the site pairs with the same color (different colors) shown in Fig. 3(b). This shows

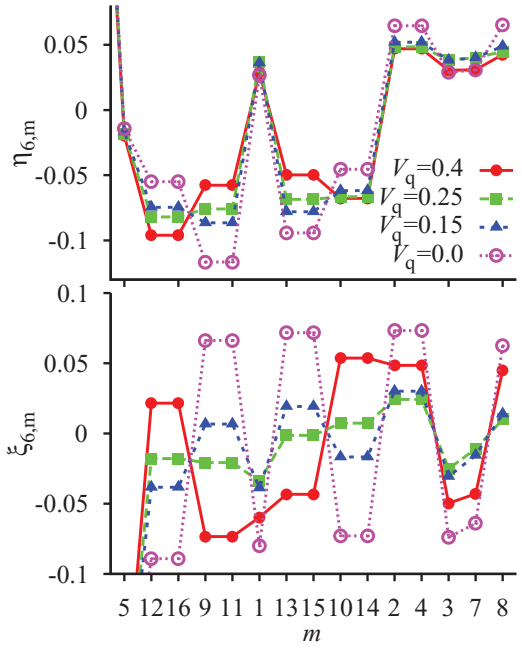

FIG. 2. (Color online) (a) The spin correlation function $\eta_{6,m}$ and (b) the charge correlation function $\xi_{6,m}$ for $V_q = 0.4$, 0.25, 0.15, and 0. The other interdimer Coulomb interaction energies are fixed to the values $V_{b2} = V_p = 0.25$.

that the charge structure shown in Fig. 3(b), where electric dipole moments in dimers are aligned along the c axis, is the dominant charge fluctuation in this case. Since the oppositely charged structure has the same quantum weight, the charge density is zero and uniform in $|\psi_0\rangle$.

As V_q is decreased from 0.45 to 0, the charge correlation function and also the other considered physical quantities change gradually, and abrupt or discontinuous changes are not observed. Furthermore, as seen from Fig. 2(a), the characteristic AFM spin correlation function of the dimer Mott insulator ground state, where the spin correlation is negative between the dimers I and II, is retained although the considered V_q region. Consequently, the ground state is the dimer Mott insulator in the considered region $0 \leqslant V_q \leqslant 0.4$. The crossover of the dominant charge fluctuation occurs as V_q changes, but the characteristic charge correlation functions in the large- and the small-V_q regions are not due to the transition to the charge-ordered states with the charge structure shown in Figs. 3(a) or 3(b).

We have also investigated the dependence of $\eta_{n,m}$ and $\xi_{n,m}$ on V_p in the range $0 \leqslant V_p \leqslant 0.4$ for $V_{b2} = V_q = 0.25$, and that on V_{b2} in the range $0 \leqslant V_{b2} \leqslant 0.4$ for $V_p = V_q = 0.25$. In these cases, the metallic state becomes the ground state in some parameter regions, but the transition to the charge-ordered phases with the charge structure shown in Figs. 3(a) or 3(b) does not occur. In the dimer Mott insulator phase, the AFM spin correlation is retained, but $\xi_{n,m}$ change remarkably also with these parameters. The charge fluctuation of the c-axis (b-axis) polarized charge structure shown in Fig. 3(b) [3(a)] is dominant in the large- (small-) V_p region. Furthermore, the dominant one of these two charge fluctuations increases as V_{b1} increases.

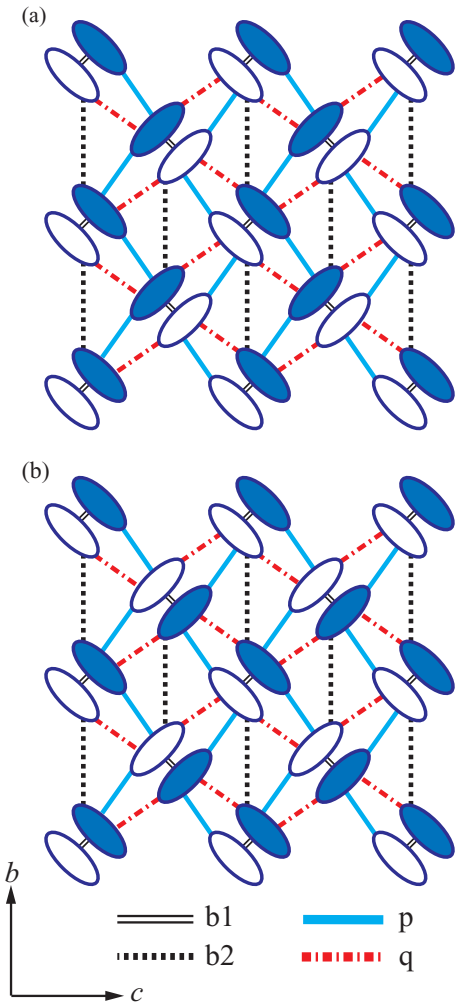

FIG. 3. (Color online) (a) Schematic representation of the charge structure where electric dipole moments in dimers are aligned along the b axis, and (b) that where the electric dipole moments in dimers are aligned along the c axis. The charge-rich and charge-poor sites are shown by the colored and white ellipsoids, respectively.

The crossover between the dominant charge fluctuations can be understood from the V_q, V_p, and V_{b2} dependencies of the Coulomb interaction energy between the dimers per dimer. It is given by $\Gamma_b \delta\rho$ ($\Gamma_c \delta\rho$) for the b-axis (c-axis) polarized charge structure shown in Fig. 3(a) [3(b)], where $\Gamma_b = 2V_p - 2V_q - V_{b2}$, $\Gamma_c = 2V_q - 2V_p - V_{b2}$, and $\delta\rho$ and $-\delta\rho$ are the charge densities at the charge-rich sites and the charge-poor sites, respectively. When Γ_b is significantly smaller (larger) than Γ_c, the b-axis (c-axis) polarized charge structure becomes the dominant charge fluctuation.

B. Electric polarization induced by bond-length alternation

In this section, we show the electronic structure of the ground state when the bond lengths alternate. We have found that aligned electric dipole moments in dimers are induced by the interdimer bond-length alternation. The interdimer bond lengths alternate along the c axis (b axis) when $\Delta x_n = \delta/2$ and $\Delta y_n = 0$ ($\Delta x_n = 0$ and $\Delta y_n = \delta/2$) hold for the dimers I and $\Delta x_n = -\delta/2$ and $\Delta y_n = 0$ ($\Delta x_n = 0$ and $\Delta y_n = -\delta/2$)

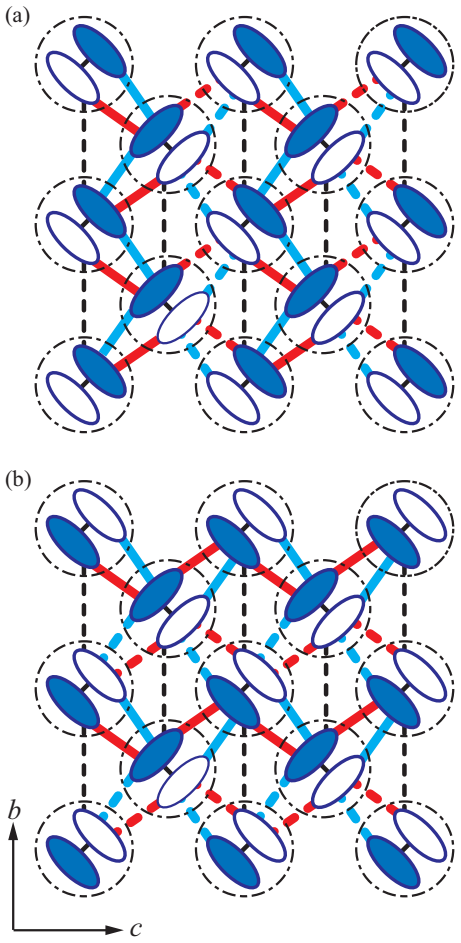

FIG. 4. (Color online) (a) The bond and charge structure when interdimer bond lengths and bond orders alternate along the c axis. The ellipsoids and circles represent the BEDT-TTF molecules and the dimers, respectively. The thick solid (thick dashed) lines show the bonds that become shorter and stronger (longer and weaker) than those in the equilibrium lattice as a result of the bond-length and bond-order alternations. The unchanged bonds are shown by the thin lines. The colored (white) ellipsoids represent the charge-rich (charge-poor) sites. (b) That when interdimer bond lengths and bond orders alternate along the b axis.

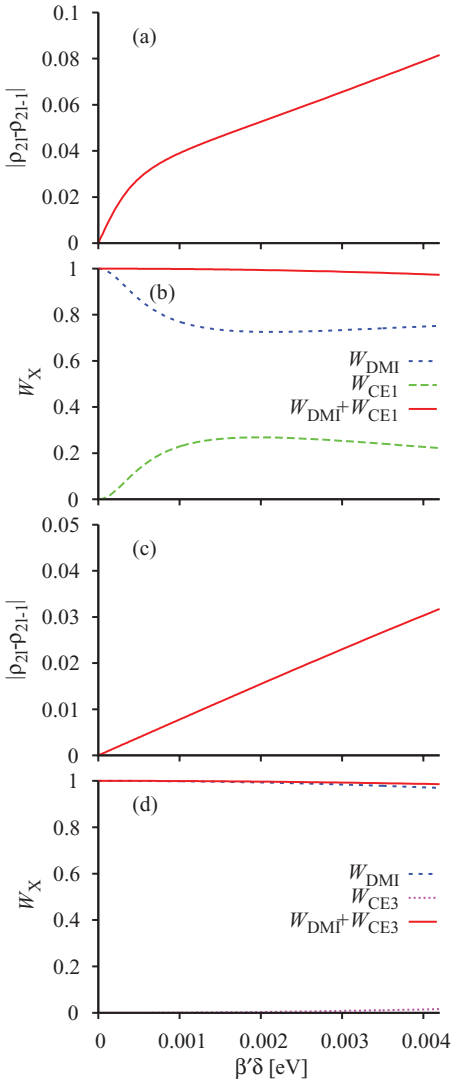

FIG. 5. (Color online) The $\beta'\delta$ dependence of (a) $|\rho_{2l}-\rho_{2l-1}|$, and (b) $W_{\rm DMI}$, $W_{\rm CE1}$, and $W_{\rm DMI}+W_{\rm CE1}$ when bond lengths alternate along the c axis. The $\beta'\delta$ dependence of (c) $|\rho_{2l}-\rho_{2l-1}|$, and (d) $W_{\rm DMI}$, $W_{\rm CE3}$, and $W_{\rm DMI}+W_{\rm CE3}$ when bond lengths alternate along the b axis. The interdimer Coulomb interaction energies $V_{\rm b2}=V_{\rm p}=V_{\rm q}=0.25$ are used.

hold for the dimers II, and δ shows the magnitude of bond-length alternation. We show the dimer lattice structure where the interdimer bond lengths alternate along the c axis (b axis) in Fig. 4(a) [4(b)]. The thick solid (thick dashed) lines show the interdimer bonds that become shorter (longer) than those in the equilibrium lattice as a result of the bond-length alternation.

We calculate the ground state in the bond-length-alternated cases for various values of $V_{\rm b2}$, $V_{\rm p}$, and $V_{\rm q}$. Irrespective of their values, the charge distribution induced by bond-length alternation is as schematically shown in Fig. 4. A site (the other site) in a dimer shown by a colored (white) ellipsoid becomes charge rich (charge poor) as a result of the alternation, but the total charge of a dimer is zero. Therefore, electric dipole moments in dimers are induced by the alternation. Furthermore, as seen from Fig. 4(a) [4(b)], the electric dipole moments are aligned along the b axis (c axis) when bond lengths alternate along the c axis (b axis). Electric polarization along the b axis (c axis) is induced by bond-length alternation along the c axis (b axis).

As mentioned before, two sites $2l-1$ and $2l$ constitute the dimer l. Therefore, $|\rho_{2l}-\rho_{2l-1}|$ shows the charge disproportionation in dimer l, and it is proportional to the electric dipole moment of the dimer. Since all the dimers are equivalent, $|\rho_{2l}-\rho_{2l-1}|$ does not depend on l. In Fig. 5, we show the $\beta'\delta$ dependence of $|\rho_{2l}-\rho_{2l-1}|$, where $\beta'\delta$ shows the change of transfer integrals by the alternation. We adopt the interdimer Coulomb interaction energies $V_{\rm b2}=V_{\rm p}=V_{\rm q}=0.25$, where $\Gamma_{\rm b}=\Gamma_{\rm c}$ holds. As seen from this figure, the charge disproportionation increases linearly to the magnitude of bond-length alternation δ in the small-δ region both in the two alternated cases along the different directions. Therefore, even very weak bond-length alternation induces electric dipole moments in dimers and electric polarization. The charge

disproportionation $|\rho_{2l} - \rho_{2l-1}|$ significantly depends on the interdimer Coulomb interaction energies. That for the b axis (c axis) ferroelectric state increases as Γ_b (Γ_c) decreases.

The origin of the electric dipole moments in dimers induced by the bond-length alternation can be understood as follows. As seen from Eq. (3), $|\beta_{n,m}|$ is larger (smaller) than $|\bar{\beta}_{n,m}|$ by $|\beta'\delta|$ for the bonds that become shorter (longer) as a result of the bond-length alternation. The expectation value of the transfer term of the Hamiltonian is given by $\sum_{\langle n,m\rangle} \beta_{n,m} p_{n,m}$, where $p_{n,m} = \langle\psi_0|\hat{p}_{n,m}|\psi_0\rangle$ is the bond order for the bond between the sites m and n, and $|p_{n,m}|$ shows the strength of the bond. To gain the transfer energy, $|p_{n,m}|$ for the shorter (longer) bonds with larger (smaller) $|\beta_{n,m}|$ become larger (smaller) than those for the equilibrium lattice. Namely, the bond orders also alternate along the same direction as that of the bond-length alternation. We confirm this from the numerical results. As a result, a site (the other site) in a dimer shown by the colored (white) ellipsoid in Fig. 4 is connected by three (one) stronger bonds and one (three) weaker bond. Since holes are more stabilized on the stronger bonds, the sites shown by the colored (white) ellipsoids become charge rich (charge poor) as a result of the bond-order alternation. Since all the dimers are equivalent even in the bond-length-alternated cases, the total charge of a dimer is zero. Furthermore, we see from the geometrical bond structure shown in Fig. 4(a) [4(b)] that the b-axis (c-axis) components of electric dipole moments in dimers are of the same sign when bond length and bond order alternate along the c axis (b axis). Electric dipole moments in dimers due to the bond-length alternation have been found also also in one-dimensional dimer Mott insulators.[11,49,50]

In the Mott insulator, all the excitations below the Mott gap are spin excitations, where charge degrees of freedom are completely frozen. On the other hand, there are in-gap charge excitations in the dimer Mott insulators.[30–32] As will be shown later, the dielectric properties are closely related to some of these in-gap charge excitations. We show the in-gap absorption spectrum $\alpha_0(\omega)$ from the ground state for the equilibrium lattice with $\Delta x_n = \Delta y_n = 0$ in Fig. 6. The Mott gap edge is at $\omega = 0.14$, and the main peaks above the gap are due to the interdimer charge-transfer excitation, where a pair of a holon (an empty dimer) and a doublon (a doubly occupied dimer) is generated.[51] As seen from this figure, there are in-gap peaks in contrast to the case of the Mott insulator. Since

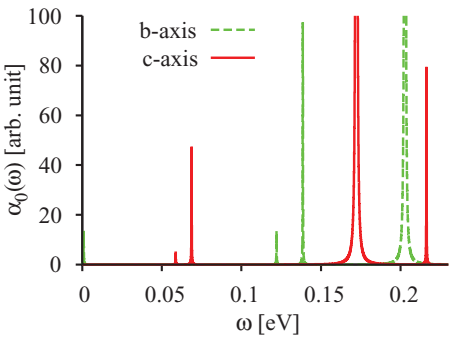

FIG. 6. (Color online) Light absorption spectrum $\alpha_0(\omega)$ when light is polarized along the b axis and that along the c axis in the equilibrium case. The interdimer Coulomb interaction energies $V_{b2} = V_p = V_q = 0.25$ are used.

these excited states are photoactive, they accompany charge motions. However, they are not interdimer charge-transfer excitations. The physical properties of these in-gap excited states will be discussed in detail in the forthcoming paper. The dimer Mott insulator ground state for the equilibrium lattice is denoted by $|\mathrm{DMI}\rangle$, and the energy eigenstate responsible to the ith lowest in-gap peak is denoted by $|\mathrm{CE}i\rangle$.

Among these in-gap excited states, $|\mathrm{CE1}\rangle$ and $|\mathrm{CE3}\rangle$ play important roles in the dielectric properties. The energy eigenstate $|\mathrm{CE1}\rangle$ is the metallic state that becomes the ground state for $\bar{\beta}_{b2} \geqslant 0.074$. The energy eigenstate $|\mathrm{CE3}\rangle$ is a dimer Mott insulator that has a different bond order and spin structure from $|\mathrm{DMI}\rangle$. In $|\mathrm{CE3}\rangle$, the bond order for the b2 bond is much larger than that for $|\mathrm{DMI}\rangle$. As a result, the spin correlation is negative between the dimers connected by the b2 bonds.

We show $W_X = |\langle X|\psi_0\rangle|^2$ in Figs. 5(b) and 5(d), where $X =$ CE1, CE3 or DMI. As seen from this figure, $W_{\mathrm{DMI}} + W_{\mathrm{CE1}}$ ($W_{\mathrm{DMI}} + W_{\mathrm{CE3}}$) is nearly equal to 1 as long as δ is small, showing that the ground state is approximately given by $|\psi_0\rangle = \sqrt{1-c^2}|\mathrm{DMI}\rangle + c|\mathrm{CE1}\rangle$ ($|\psi_0\rangle = \sqrt{1-c^2}|\mathrm{DMI}\rangle + c|\mathrm{CE3}\rangle$) when bond lengths alternate along the c axis (b axis). Here, c is a real constant. The slight hybridization of the in-gap excited state induces bond-order alternation and the electric polarization. As the magnitude of bond alternation δ increases, the hybridization increases and the magnitude of electric dipole moment increases.

The origins of these two polarized states induced by bond-order alternation are different from those of conventional charge-ordered states stabilized by direct interdimer Coulomb interactions. This can be confirmed from the numerical result that the polarized states are generated by bond-length alternation even in the case of $V_{b2} = V_p = V_q = 0$, where stabilization by the interdimer Coulomb interaction is not taken into account.

C. Polarization induced by disorder

We consider the effects of the disorder in this section. For the purpose, we consider a large number of samples of disordered lattices. A sample of a disordered lattice is determined from two sets of $N/2$ random numbers $\{r_l\}$ and $\{s_l\}$ that satisfy the conditions $\langle r_l\rangle = \langle s_l\rangle = 0$ and $\beta'\langle|r_l|\rangle = \beta'\langle|s_l|\rangle = \Delta$, where $\langle r_l\rangle = (2/N)\sum_{l=1}^{N/2} r_l$ denotes the average value. Using these random numbers, lattice deviations for the sample are given by $\Delta x_{2l-1} = \Delta x_{2l} = r_l$, and $\Delta y_{2l-1} = \Delta y_{2l} = s_l$, for $l = 1,2,\ldots,(N/2)$. As seen from Eq. (3), Δ gives the rough estimation of the magnitudes of the random deviations in the interdimer transfer integrals.

As shown before, the charge fluctuations of the ground state for the equilibrium lattice strongly depend on V_{b2}, V_p, and V_q, and the dependence can be understood from the values of Γ_b and Γ_c. The dependence of the effects of disorder on V_{b2}, V_p, and V_q can be understood also from these values. Since these two values can be controlled by changing, for example, V_p, we show only the V_q dependence of them. We first show the results for $V_{b2} = V_p = V_q = 0.25$, where $\Gamma_b = \Gamma_c$ holds.

Before showing the distribution of the considered physical quantities to the samples, we first consider the Δ dependence of charge distribution for a single sample, where the lattice displacements with different Δ are given by scaling of two

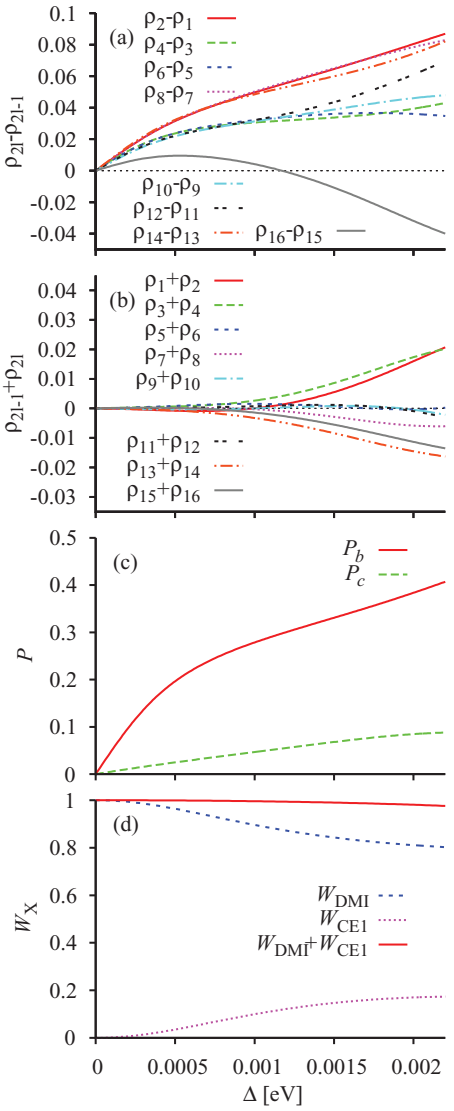

FIG. 7. (Color online) The Δ dependence of (a) $\rho_{2l} - \rho_{2l-1}$, (b) $\rho_{2l-1} + \rho_{2l}$, (c) P_b and P_c, and (d) $W_{\rm DMI}$, $W_{\rm CE1}$, and $W_{\rm DMI} + W_{\rm CE1}$. The interdimer Coulomb interaction energies $V_{\rm b2} = V_{\rm p} = V_{\rm q} = 0.25$ are used.

sets of random numbers. That is, we adopt only two sets of random numbers $\{\tilde{r}_n\}$ and $\{\tilde{s}_n\}$ that satisfies the conditions $\langle\tilde{r}_n\rangle = \langle\tilde{s}_n\rangle = 0$ and $\beta'\langle|\tilde{r}_n|\rangle = \beta'\langle|\tilde{s}_n|\rangle = 1$, and the lattice displacements with Δ are given by $\Delta x_{2l-1} = \Delta x_{2l} = \Delta\tilde{r}_n$, and $\Delta y_{2l-1} = \Delta y_{2l} = \Delta\tilde{s}_n$. In Figs. 7(a) and 7(b), we show the Δ dependence of $\rho_{2l} - \rho_{2l-1}$ and $\rho_{2l-1} + \rho_{2l}$, respectively. Here, the results of only one sample are shown. However, since we adopt a typical sample as will be mentioned later, the following results hold qualitatively for most of the investigated samples. Furthermore, they can be also confirmed by analyzing the distribution of the considered physical quantities to the samples as will be shown later.

As seen from these figures, the crossover of the charge density distribution occurs around a crossover magnitude of disorder $\Delta_{\rm c}$. The value $\Delta_{\rm c}$ depends on the parameters and also on the samples, and $\Delta_{\rm c} = 0.0007$ in the present case. We first consider the weak disorder case $\Delta \lesssim \Delta_{\rm c}$. Since two sites $2l-1$ and $2l$ constitute the dimer l, $\rho_{2l-1} + \rho_{2l}$ shows the total charge of the dimer l, and $|\rho_{2l} - \rho_{2l-1}|$ shows the magnitude of intradimer charge transfer in the dimer l. As seen from Figs. 7(a) and 7(b), $|\rho_{2l-1} + \rho_{2l}|$ are much smaller than $|\rho_{2l} - \rho_{2l-1}|$. This shows that interdimer charge transfer is negligible, and the electric dipole moments in dimers are generated in $|\psi_0\rangle$.

Furthermore, $\rho_{2l} - \rho_{2l-1} > 0$ holds for all l in contrast to $\rho_{2l-1} + \rho_{2l}$ with random signs. As seen from the definition of the site numbers shown in Fig. 1, the b-axis component of the electric dipole moment in the dimer l is given by $(\rho_{2l} - \rho_{2l-1})l_b e$, and the c-axis component is given by $(\rho_{2l} - \rho_{2l-1})l_c e$ for $l \leqslant 4$ and $-(\rho_{2l} - \rho_{2l-1})l_c e$ for $l \geqslant 5$, where l_b (l_c) is the projection length of the b1 bond on the b axis (c axis), and e is the elementary charge. Therefore, the present result shows that the b-axis components of all the electric dipole moments in dimers are of the same sign, and $|\psi_0\rangle$ has the charge distribution schematically shown in Fig. 4(a). The electric polarization along the b axis is generated in $|\psi_0\rangle$ in spite of the fact that these electric dipole moments are generated by disorder.

We consider the sum of the b-axis (c-axis) components of the electric dipole moments in dimers P_b (P_c), which is given by $P_b = \sum_{l=1}^{8}\{\rho_{2l} - \rho_{2l-1}\}$ ($P_c = \sum_{l=1}^{4}\{\rho_{2l} - \rho_{2l-1}\} - \sum_{l=5}^{8}\{\rho_{2l} - \rho_{2l-1}\}$). We show the Δ dependence of P_b and P_c in Fig. 7(c). The electric dipole moments in dimers are aligned along the b axis, and their magnitudes increase as Δ increases as seen from Fig. 7(a). As a result, the b-axis component of the electric polarization P_b increases as Δ increases as shown in Fig. 7(c).

To consider the origin of the ordering of the electric dipole moments in dimers, we show the Δ dependence of $W_X = |\langle X|\psi_0(\Delta)\rangle|^2$ in Fig. 7(d), where $X =$ CE1 or DMI. As seen from this figure, $W_{\rm DMI} + W_{\rm CE1}$ is equal to 1 almost precisely for $\Delta < \Delta_{\rm c}$. This shows that the ground state for the disordered lattice is approximately given by $|\psi_0\rangle = \sqrt{1-c^2}|{\rm DMI}\rangle + c|{\rm CE1}\rangle$ just like the case of the ground state for the bond-length-alternated lattice along the c axis. Therefore, disorder also induces bond-order alternation along the c axis, and this results in electric polarization along the b axis. Furthermore, the origin of the b-axis polarized state is also different from that of a conventional charge-ordered state stabilized by direct interdimer Coulomb interactions. Since the electric dipole moments in dimers are generated by the hybridization of two uniform states in space, their directions do not distribute randomly but they are aligned along the b axis.

We next consider the strong disorder region $\Delta \gtrsim \Delta_{\rm c}$. The characteristic charge structure in the weak disorder region is not seen in the region as seen from Fig. 7. The deviations of $\rho_{2l} - \rho_{2l-1}$ for different l become larger as Δ increases, showing that the distribution of electric dipole moments in dimers becomes more random as Δ increases. As a result, $|dP_b/d\Delta|$ in the region is significantly smaller than that in the weak disorder region. Furthermore, $|\rho_{2l-1} + \rho_{2l}|$ increase as Δ increases and become comparable to $|\rho_{2l} - \rho_{2l-1}|$ around $\Delta = 0.002$. The charge structure for $\Delta \gtrsim 0.002$ can not be described well by the electric dipole moments in dimers. As seen from Fig. 7(d), $W_{\rm DMI} + W_{\rm CE1}$ decreases with increasing

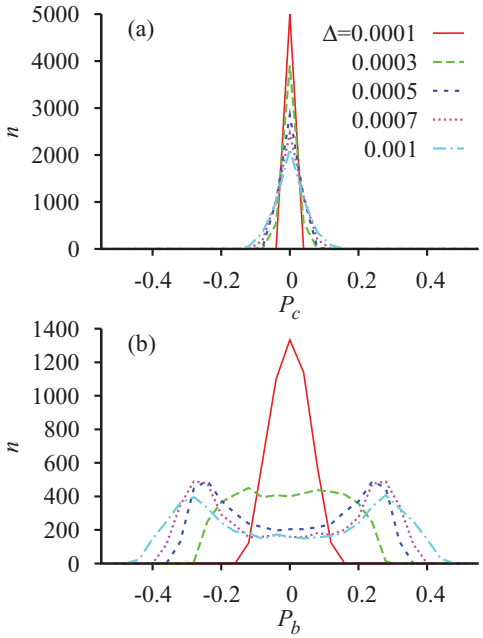

FIG. 8. (Color online) (a) The histogram of P_c and (b) that of P_b for the various values of Δ. The interdimer Coulomb interaction energies $V_{b2} = V_p = V_q = 0.25$ are used.

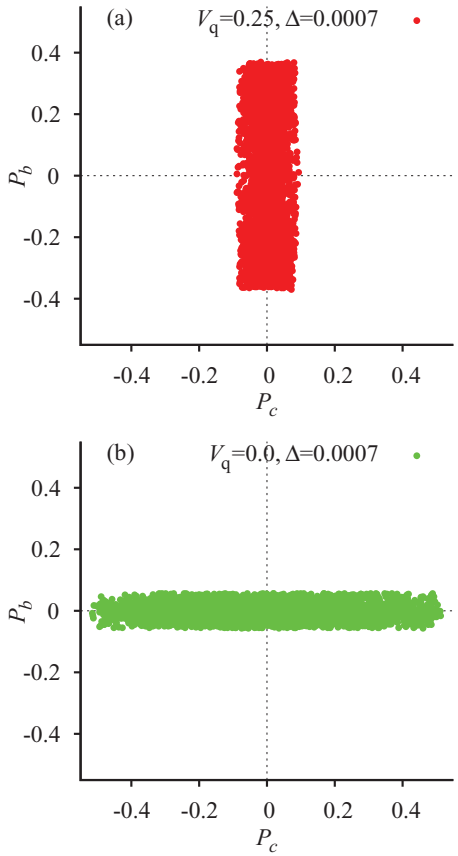

FIG. 9. (Color online) (a) The scatter plot of P_b versus P_c for $\Delta = 0.0007$. The interdimer Coulomb interaction energies $V_{b2} = V_p = V_q = 0.25$ are used. (b) A scatter plot of P_b versus P_c for $\Delta = 0.0007$. The interdimer Coulomb interaction energies $V_{b2} = V_p = 0.25$ and $V_q = 0$ are used.

Δ in the region, and the deviation from 1 becomes significant, showing that the ground state is not approximated well by the hybridized state in the stronger disorder region. As a result, the characteristic electronic structure in the weak disorder region, which arises from the hybridization, is not seen in the region.

We next consider the distribution of P_b and P_c for a large number of samples of disordered lattices. We consider 5000 samples for each value of Δ. We show the histogram of P_b and that of P_c in Fig. 8, and the scatter plot of P_b versus P_c in Fig. 9(a).

As seen from Fig. 8, the histogram of P_b is essentially different from Gaussian distribution. A standard deviation of P_b increases significantly with increasing Δ for $\Delta \lesssim 0.0007$, and the single peak centered at $P_b = 0$ for $\Delta = 0.0001$ splits into two peaks at the positive and negative values for $\Delta \gtrsim 0.0003$. The absolute values of the two peak positions are nearly the same, and they increase as Δ increases for $\Delta \lesssim 0.0007$. These characteristic behaviors are not seen in the histogram of P_c. There is a single peak, and the peak just becomes broader as Δ increases. Furthermore, the standard deviation of P_b is about seven times as large as that of P_c, for example, around $\Delta = 0.0007$. As seen from the scatter plot of P_b versus P_c for $\Delta = 0.0007$ shown in Fig. 9(a), the distribution is far from the isotropic one, which is expected when electric dipole moments distribute randomly in space. These results clearly show that electric dipole moments in dimers are aligned along the b axis for most of the samples for $\Delta \lesssim 0.0007$, and the characteristic distributions of P_b and P_c and their Δ dependence can be explained well from the charge structure in the weak disorder region shown before.

For $\Delta \gtrsim 0.0007$, the absolute values of the two peak positions are nearly constant to Δ, and the two peaks become broader as Δ increases. This can be explained well from the charge structure in the strong disorder region. As mentioned before, Δ_c differs for the different samples, and the samples that have larger $|P_b|$ tend to have larger Δ_c. Since the sample shown in Fig. 7 gives P_b and P_c nearly equal to their peak values in their histograms, respectively, we can say that the sample is a typical one. The Δ dependence of the histogram shows that the crossover between the weaker and stronger disorder regions occurs around $\Delta = 0.0007$ for most of the samples. Therefore, the characteristic distribution of P_b and its Δ dependence for $\Delta \lesssim 0.0007$ are attributed to the properties of the hybridized state $\sqrt{1-c^2}|\mathrm{DMI}\rangle + c|\mathrm{CE1}\rangle$.

The electric dipole moments in dimers are aligned along the b axis for most of the samples, but the signs of P_b are randomly distributed. The sign of P_b is determined from the phase of bond-order alternation. There are two phases of bond-order (-length) alternation along each direction. The phase of the bond-order (-length) alternation shown in Fig. 4 is defined as the phase A. In the other phase B, stronger (shorter) and weaker (longer) bonds are reversed from those in the phase A. Furthermore, the charge-rich and the charge-poor sites are also reversed from each other between these two phases. Therefore, $P_b > 0$ ($P_b < 0$) holds when bond orders alternate along the c axis with the phase A (B). Since the bond-order alternation and electric polarization for the hybridized state $\sqrt{1-c^2}|\mathrm{DMI}\rangle + c|\mathrm{CE1}\rangle$ arise from the off-diagonal part between $|\mathrm{DMI}\rangle$ and

$|\mathrm{CE1}\rangle$, the phase of bond-order alternation and therefore the sign of P_b are determined from the sign of c. As will be shown later, the signs of c are randomly distributed, which results in the random signs of P_b.

Various energy eigenstates are hybridized to $|\mathrm{DMI}\rangle$ by the perturbation of random lattice displacements. However, the hybridization of $|\mathrm{CE1}\rangle$ is by far the largest among them for most of the samples. We next consider the cause of this result. Numerical results show that there is a strong positive correlation between P_b and $\Delta x(\pi,0)$, where $\Delta x(\pi,0)$ is the Fourier transformation of dimer lattice displacements with the wave number $(\pi,0)$, and it is given by $\Delta x(\pi,0) = \sum_{l=1}^{4} \Delta x_{2l} - \sum_{l=5}^{8} \Delta x_{2l}$. The quantity of $|\Delta x(\pi,0)|$ shows the magnitude of the Fourier component that corresponds to the bond-length alternation along the c axis, and the sign of $\Delta x(\pi,0)$ shows the phase of the alternation, for a sample of random lattices.

Since P_b arises from the hybridization of $|\mathrm{CE1}\rangle$, this result shows strong correlation also between the hybridization and $\Delta x(\pi,0)$. Therefore, the hybridization is mainly due to the Fourier component $\Delta x(\pi,0)$, and the contributions of the other components are negligible. This can be attributed to the fact that the hybridized state $\sqrt{1-c^2}|\mathrm{DMI}\rangle + c|\mathrm{CE1}\rangle$, where bond orders alternate along the c axis, is strongly stabilized by the bond-length alternation along the same direction with the same phase. Furthermore, the energy eigenvalues for the metallic state $|\mathrm{CE1}\rangle$ and the dimer Mott ground state $|\mathrm{DMI}\rangle$ are very close to each other with the present parameters, which are near the phase boundary between these two phases. As a result, the hybridization of $|\mathrm{CE1}\rangle$ due to the Fourier component $\Delta x(\pi,0)$ is by far the largest compared with the other combinations of an energy eigenstate and a lattice mode.

Bond orders alternate along the b axis in the hybridized state $\sqrt{1-c^2}|\mathrm{DMI}\rangle + c|\mathrm{CE3}\rangle$, and the state is also strongly stabilized by the bond-length alternation along the same direction with the same phase. Therefore, the hybridization of $|\mathrm{CE3}\rangle$ due to the Fourier component $\Delta y(0,\pi)$, which corresponds to the bond-length alternation along the b axis, is also large. However, the coupling between the hybridization of $|\mathrm{CE1}\rangle$ and the lattice mode of $\Delta x(\pi,0)$ is significantly larger than that between the hybridization of $|\mathrm{CE3}\rangle$ and the lattice mode of $\Delta y(0,\pi)$ for the present parameters. This can be seen from the results shown in Figs. 5(b) and 5(d). The hybridization for a given δ is much larger in the case of c-axis bond-length alternation than in the case of the b-axis one. The magnitudes of the couplings strongly depend on the interdimer Coulomb interactions. This point will be discussed later.

As a result of the especially strong coupling between the hybridization of $|\mathrm{CE1}\rangle$ and lattice mode of $\Delta x(\pi,0)$, the hybridization of $|\mathrm{CE1}\rangle$ is dominant except for the few samples where $|\Delta x(\pi,0)|$ is very small. This is the reason why the electric polarization is induced by the lattice disorder for most of the samples. Furthermore, as the energy difference Δe between these two states decreases, the hybridization increases. As a result, the effects of disorder are enhanced near the phase boundary between the dimer Mott insulator and the metallic phases. The hybridized state with the phase A (B) of bond-order alternation becomes the electronic ground state when $\Delta x(\pi,0) > 0$ $[\Delta x(\pi,0) < 0]$ holds. Since the signs of

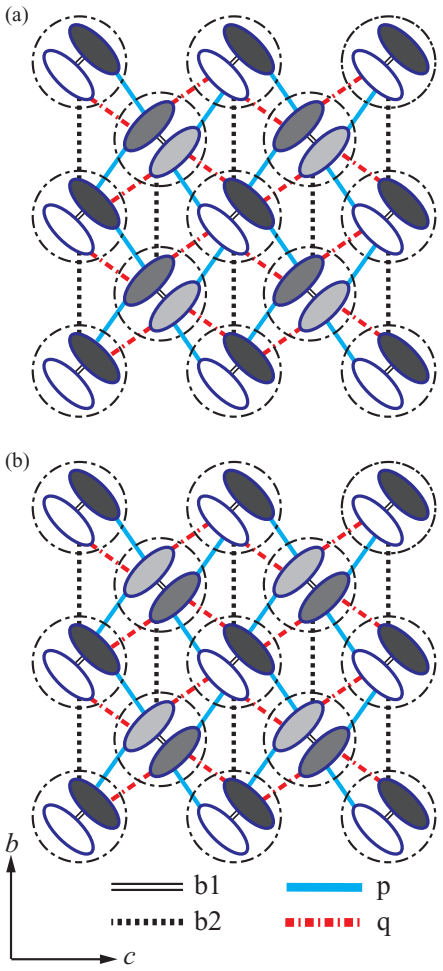

FIG. 10. (Color online) Schematic representation of the charge structure that has large $|P_b|$ and $|P_c|$ simultaneously in the cases (a) $|P_b| > |P_c|$ and (b) $|P_b| < |P_c|$, where the BEDT-TTF molecules and dimers are shown by the ellipsoid and circles, respectively, and the charges are larger at the sites with darker colors.

$\Delta x(\pi,0)$ are randomly distributed, the phases of bond-order alternation and therefore the signs of P_b are random.

We next show the results with $V_{\mathrm{b2}} = V_{\mathrm{p}} = 0.25$ and $V_{\mathrm{q}} = 0$, where $\Gamma_{\mathrm{c}} \ll \Gamma_{\mathrm{b}}$ holds. We show the scatter plot of P_b versus P_c for $\Delta = 0.0007$ in Fig. 9(b). As seen from this figure, a standard deviation of P_c is much larger than that of P_b in contrast to the case of $V_{\mathrm{b2}} = V_{\mathrm{p}} = V_{\mathrm{q}} = 0.25$. From the same analysis of this result and others as the case of $V_{\mathrm{q}} = 0.25$, we can show the following results in the weaker disorder region. The ground states for the disordered lattices are approximately given by the linear combination of $|\mathrm{DMI}\rangle$ and $|\mathrm{CE3}\rangle$ for most of the samples. In the hybridized state $\sqrt{1-c^2}|\mathrm{DMI}\rangle + c|\mathrm{CE3}\rangle$, the bond orders alternate along the b axis, and the bond-order alternation induces electric dipole moments in dimers aligned along the c axis. The electric polarization along the c axis is induced by disorder when Γ_{c} is significantly smaller than Γ_{b}.

As V_{q} is decreased from 0.25, the quantum weight of $|\mathrm{CE1}\rangle$ in the disordered ground state decreases and that of $|\mathrm{CE3}\rangle$ increases, and the crossover between the b- and c-axis polarized states occurs around $V_{\mathrm{q}} = 0.15$. The physical

properties of some in-gap excited states strongly depend on the interdimer Coulomb interactions. As a result, the electron-lattice coupling between the hybridization of $|\mathrm{CE3}\rangle$ and lattice mode of $\Delta y(0,\pi)$ increases significantly as V_q decreases. This is the cause of the crossover. This problem will be discussed in a forthcoming paper.

In the crossover region, the quantum weight of $|\mathrm{CE1}\rangle$ and that of $|\mathrm{CE3}\rangle$ are both significant, and both $|P_b|$ and $|P_c|$ are large in $|\psi_0\rangle$ for the most of the samples. In the ground state in the crossover region, large $|P_b|$ and large $|P_c|$ are compatible in the following way. When $|P_b|$ is larger (smaller) than $|P_c|$, the electric dipole moments in dimers are aligned along the b axis (c axis), and their magnitudes in the dimers I are much larger than those in the dimers II, as schematically shown in Fig. 10(a) [10(b)]. When V_q is larger than 0.25, and $\Gamma_\mathrm{b} \ll \Gamma_\mathrm{c}$ holds, the disordered ground state is the hybridized state $\sqrt{1-c^2}|\mathrm{DMI}\rangle + c|\mathrm{CE1}\rangle$, and the state has the electric polarization along the b axis just like the case of $V_\mathrm{q} = 0.25$. The magnitude of polarization increases as V_q increases and Γ_b decreases.

IV. DISCUSSION

First, we compare present results with those obtained in the effective Hamiltonians for the strong on-dimer Coulomb interaction case.[38,39] The bond orders for the interdimer bonds arise from the hybridization between the states that have no doubly occupied dimers and those with a doubly occupied dimer. Therefore, their magnitudes decrease as on-dimer Coulomb interaction energy $U^{(\mathrm{dim})}$ increases. As a result, the coupling between electric dipole moments in dimers and lattice becomes smaller as $U^{(\mathrm{dim})}$ increases, but qualitatively the same results are obtained in the present model even when we use quite different values of $U^{(\mathrm{dim})}$ as long as the ground state is the dimer Mott insulator. Since the Hilbert space is restricted to the states where there is one hole in each dimer, interdimer bond orders are zero, and the interdimer bond-order alternation can not be described in these effective Hamiltonians. However, since the spin-spin coupling included in these models is induced by these virtual excited states that have a doubly occupied dimer, interdimer bond order and interdimer spin correlation are strongly correlated. Actually, the AF spin correlation is larger for the stronger bond in the bond-order-alternated states. Therefore, the states with alternated interdimer spin correlations are the equivalents in the effective models of the bond-order-alternated states obtained in the present model. Since alternation of the spin correlation is not observed in the ferroelectric states found, we consider that their origins are different from those found in the present model. Furthermore, in the present model, the ferroelectric ground state is not obtained even in the parameter range where the ferroelectric phase appears in these effective models. In these parameter ranges where ferroelectric states are strongly stabilized, a metallic state is also stabilized and the metallic state becomes the ground state.

We next consider the effect of dimer lattice disorder on the spin-liquid state. As shown in the previous section, the c-axis ferroelectric state is induced by hybridization of the dimer Mott insulator state $|\mathrm{CE3}\rangle$ with different bond order and spin structures from those for the dimer Mott insulator ground state. In the spin-liquid state, there are almost degenerate dimer Mott insulator states with different spin structures, and the energy difference between $|\mathrm{DMI}\rangle$ and $|\mathrm{CE3}\rangle$ will be very small. Therefore, the hybridization among them and the electric polarization along the c axis induced by disorder will be very large in the spin-liquid state. This problem will be discussed in a forthcoming paper.

We next show the implications of the present results for the dielectric anomaly in κ-(BEDT-TTF)$_2$Cu$_2$(CN)$_3$. A broad peak has been observed around 25 K in the temperature dependence of the dielectric constant, which shows a relaxor ferroelectriclike behavior.[13] Based on the present results, these results can be explained in the following way. We consider that the randomness in dimer lattice is induced by thermal fluctuations. We first consider the correspondence between the temperature T and the magnitude of disorder Δ. For a simplicity, we assume that the deformation energy for a bond is given by $(1/2)\kappa(\Delta/\beta')^2$ using a single spring constant κ for all the bonds. In this case, the following relation holds: $T = 5\kappa(\Delta/\beta')^2$, where we use the fact that there are five bonds per dimer.

As mentioned before, it is expected that the polarization along the c axis is dominant in the spin-liquid state κ-(BEDT-TTF)$_2$Cu$_2$(CN)$_3$. In case of the weak disorder $T \lesssim T_c$, the polarization $|P_c|$ increases as T increases as shown in the previous section. For $T > T_c$ and $T \simeq T_c$, $|P_c|$ is roughly constant to T. We have considered only the disorder in dimer lattice as an effect of thermal fluctuations. However, the other effects become important in the region, and the thermal fluctuations will weaken the ferroelectric order. Therefore, the polarization will become maximum around $T = T_c$, and this T dependence of polarization is consistent with the experimental results. The polarization will become maximum around $T = T_c$ also in the b-axis ferroelectric case.

Since the effects of dimer lattice disorder significantly depend on $\Delta e'$, we need to estimate its reasonable value to compare the present results with the experimental data quantitatively. Unfortunately, it is difficult to estimate it from experimental data. For example, in the case of $V_\mathrm{q} = 0$, where c-axis polarization is dominant, $\Delta_\mathrm{c} = 0.005$ and this value corresponds to $T_c = 5\kappa(\Delta/\beta')^2 = 29$ K if we use the value $\kappa/(\beta')^2 = 20$ for the b2 bond of charge-ordered insulator α-(BEDT-TTF)$_2$I$_3$ as a rough estimation.[46] The charge disproportionation around $\Delta = \Delta_c$ is about $0.04e$.

When Δe or $\Delta e'$ is very small, even very small disorder induces polarization. For example, the value $\Delta_\mathrm{c} = 0.0007$ for $V_\mathrm{q} = 0.25$ corresponds to $T_c = 0.5$ K. Furthermore, the spontaneous symmetry breaking of bond-length alternation occurs, and the ferroelectric state becomes the ground state without disorder in this case as shown before. The anomaly around 6 K (Refs. 36 and 37) may be related to this spontaneous symmetry breaking.

Electric dipole moments in dimers are proposed also in the other dimer Mott insulators with small geometrical frustration such as β'-(BEDT-TTF)$_2$ICl$_2$.[14] The electric dipole moments in dimers are induced by dimer lattice disorder even in the dimer Mott insulators with small or no geometrical frustration. For example, we have numerically calculated the ground state for one-dimensional dimer Mott insulator with dimer lattice disorder, and have found that the disorder induces electric

dipole moments in dimers also in the one-dimensional case with no frustration. Since the ferroelectric state that arises from the hybridization of the dimer Mott insulators with different spin structure is strongly stabilized in the spin-liquid phase as mentioned before, the state will be strongly stabilized by frustration. On the other hand, the frustration does not stabilize the ferroelectric state that results from hybridization of the metallic state. Near the phase boundary between the dimer Mott insulator and the metallic phases, the geometrical frustration has almost no effect on the electronic polarization.

V. CONCLUSION

In summary, electric dipole moments in dimers aligned along the b axis (c axis) are induced by interdimer bond-order alternation along the c axis (b axis) in the dimer Mott insulator phase with the lattice structure of κ-(BEDT-TTF)$_2X$. As a result, the electric polarizations arising from the electric dipole moments in dimers are strongly coupled with the dimer lattice modes of interdimer bond-length alternation, and the more stable one of these two ferroelectric states is induced by disorder in the dimer lattice. The ferroelectric state along the b axis (c axis) arises from the hybridization of a metallic state (another dimer Mott insulator state) to the dimer Mott ground state for equilibrium lattice. Therefore, the ferroelectric state along the b axis (c axis) is strongly stabilized near the phase boundary with the metallic phase (in the spin-liquid phase). The present results are consistent with the experimentally observed dielectric anomaly in κ-(BEDT-TTF)$_2$Cu$_2$(CN)$_3$.

[1] J. van den Brink and D. I. Khomskii, J. Phys.: Condens. Matter **20**, 434217 (2008).
[2] S. Ishihara, J. Phys. Soc. Jpn. **79**, 011010 (2010).
[3] T. Kimura, T. Goto, H. Shintani, K. Ishizaka, T. Arima, and Y. Tokura, Nature (London) **426**, 55 (2003).
[4] J. Wang, J. B. Neaton, H. Zheng, V. Nagarajan, S. B. Ogale, B. Liu, D. Viehland, V. Vaithyanathan, D. G. Schlom, U. V. Waghmare, N. A. Spaldin, K. M. Rabe, M. Wuttig, and R. Ramesh, Science **299**, 1719 (2003).
[5] P. Lunkenheimer, J. Müller, S. Krohns, F. Schrettle, A. Loidl, B. Hartmann, R. Rommel, M. de Souza, C. Hotta, J. A. Schlueter, and M. Lang, Nat. Mater. **11**, 755 (2012).
[6] N. Ikeda, H. Ohsumi, K. Ohwada, K. Ishii, T. Inami, K. Kakurai, Y. Murakami, K. Yoshii, S. Mori, Y. Horibe, and H. Kito, Nature (London) **436**, 1136 (2005).
[7] A. Nagano, M. Naka, J. Nasu, and S. Ishihara, Phys. Rev. Lett. **99**, 217202 (2007).
[8] M. Naka, A. Nagano, and S. Ishihara, Phys. Rev. B **77**, 224441 (2008).
[9] P. Monceau, F. Ya. Nad, and S. Brazovskii, Phys. Rev. Lett. **86**, 4080 (2001).
[10] H. Yoshioka, M. Tsuchiizu, and H. Seo, J. Phys. Soc. Jpn. **76**, 103701 (2007).
[11] Y. Otsuka, H. Seo, Y. Motome, and T. Kato, J. Phys. Soc. Jpn. **77**, 113705 (2008).
[12] K. Yamamoto, S. Iwai, S. Boyko, A. Kashiwazaki, F. Hiramatsu, C. Okabe, N. Nishi, and K. Yakushi, J. Phys. Soc. Jpn. **77**, 074709 (2008).
[13] M. Abdel-Jawad, I. Terasaki, T. Sasaki, N. Yoneyama, N. Kobayashi, Y. Uesu, and C. Hotta, Phys. Rev. B **82**, 125119 (2010).
[14] S. Iguchi, S. Sasaki, N. Yoneyama, H. Taniguchi, T. Nishizaki, and T. Sasaki, Phys. Rev. B **87**, 075107 (2013).
[15] H. Kino and H. Fukuyama, J. Phys. Soc. Jpn. **64**, 2726 (1995).
[16] H. Kino and H. Fukuyama, J. Phys. Soc. Jpn. **65**, 2158 (1996).
[17] H. C. Kandpal, I. Opahle, Y.-Z. Zhang, H. O. Jeschke, and R. Valentí, Phys. Rev. Lett. **103**, 067004 (2009).
[18] K. Nakamura, Y. Yoshimoto, T. Kosugi, R. Arita, and M. Imada, J. Phys. Soc. Jpn. **78**, 083710 (2009).
[19] B. J. Powell and R. H. McKenzie, Rep. Prog. Phys. **74**, 056501 (2011).
[20] Y. Shimizu, K. Miyagawa, K. Kanoda, M. Maesato, and G. Saito, Phys. Rev. Lett. **91**, 107001 (2003).
[21] S. Yamashita, Y. Nakazawa, M. Oguni, Y. Oshima, H. Nojiri, Y. Shimizu, K. Miyagawa, and K. Kanoda, Nat. Phys. **4**, 459 (2008).
[22] M. Yamashita, N. Nakata, Y. Kasahara, T. Sasaki, N. Yoneyama, N. Kobayashi, S. Fujimoto, T. Shibauchi, and Y. Matsuda, Nat. Phys. **5**, 44 (2009).
[23] A. P. Ramirez, Nat. Phys. **4**, 442 (2008).
[24] T. Komatsu, N. Matsukawa, T. Inoue, and G. Saito, J. Phys. Soc. Jpn. **65**, 1340 (1996).
[25] H. Morita, S. Watanabe, and M. Imada, J. Phys. Soc. Jpn. **71**, 2109 (2002).
[26] T. Koretsune, Y. Motome, and A. Furusaki, J. Phys. Soc. Jpn. **76**, 074719 (2007).
[27] T. Yoshioka, A. Koga, and N. Kawakami, Phys. Rev. Lett. **103**, 036401 (2009).
[28] B. Kyung and A.-M. S. Tremblay, Phys. Rev. Lett. **97**, 046402 (2006).
[29] R. T. Clay, H. Li, and S. Mazumdar, Phys. Rev. Lett. **101**, 166403 (2008).
[30] H. Gomi, T. Imai, A. Takahashi, and M. Aihara, Phys. Rev. B **82**, 035101 (2010).
[31] K. Itoh, H. Itoh, M. Naka, S. Saito, I. Hosako, N. Yoneyama, S. Ishihara, T. Sasaki, and S. Iwai, Phys. Rev. Lett. **110**, 106401 (2013).
[32] M. Naka and S. Ishihara, J. Phys. Soc. Jpn. **82**, 023701 (2012).
[33] Y. Shimizu, K. Miyagawa, K. Kanoda, M. Maesato, and G. Saito, Phys. Rev. B **73**, 140407(R) (2006).
[34] A. Kawamoto, Y. Honma, K.-I. Kumagai, N. Matsunaga, and K. Nomura, Phys. Rev. B **74**, 212508 (2006).
[35] S. Nakajima, T. Suzuki, Y. Ishi, K. Ohishi, I. Watanabe, T. Goto, A. Oosawa, N. Yoneyama, N. Kobayashi, F. Pratt, and T. Sasaki, J. Phys. Soc. Jpn. **81**, 093706 (2012).
[36] M. de Souza, A. Brühl, Ch. Strack, B. Wolf, D. Schweitzer, and M. Lang, Phys. Rev. Lett. **99**, 037003 (2007).
[37] R. S. Manna, M. de Souza, A. Brühl, J. A. Schlueter, and M. Lang, Phys. Rev. Lett. **104**, 016403 (2010).
[38] M. Naka and S. Ishihara, J. Phys. Soc. Jpn. **79**, 063707 (2010).
[39] C. Hotta, Phys. Rev. B **82**, 241104 (2010).

[40]K. Sedlmeier, S. Elsasser, D. Neubauer, R. Beyer, D. Wu, T. Ivek, S. Tomic, J. A. Schlueter, and M. Dressel, Phys. Rev. B **86**, 245103 (2012).
[41]S. Tomić, M. Pinterić, T. Ivek, K. Sedlmeier, R. Beyer, D. Wu, J. A. Schlueter, D. Schweitzer, and M. Dressel, arXiv:1210.3566.
[42]S. Dayal, R. T. Clay, H. Li, and S. Mazumdar, Phys. Rev. B **83**, 245106 (2011).
[43]H. Seo, J. Phys. Soc. Jpn. **69**, 805 (2000).
[44]T. Mori, H. Mori, and S. Tanaka, Bull. Chem. Soc. Jpn. **72**, 179 (1999).
[45]S. Miyashita and K. Yonemitsu, Phys. Rev. B **75**, 245112 (2007).
[46]Y. Tanaka and K. Yonemitsu, J. Phys. Soc. Jpn. **77**, 094712 (2008).
[47]E. Scriven and B. J. Powell, J. Chem. Phys. **130**, 104508 (2009).
[48]E. Scriven and B. J. Powell, Phys. Rev. B **80**, 205107 (2009).
[49]R. T. Clay, S. Mazumdar, and D. K. Campbell, Phys. Rev. B **67**, 115121 (2003).
[50]M. Kuwabara, H. Seo, and M. Ogata, J. Phys. Soc. Jpn. **72**, 225 (2003).
[51]T. Tatsumi, H. Gomi, A. Takahashi, Y. Hirao, and Masaki Aihara, J. Phys. Soc. Jpn. **81**, 034712 (2012).